AN APPROXIMATION FOR THE rp-PROCESS

Felix Rembges, Christian Freiburghaus, Thomas Rauscher, Friedrich-Karl Thielemann

Departement für Physik und Astronomie, Universität Basel, CH-4056 Basel, Switzerland; http://quasar.physik.unibas.ch/

Hendrik Schatz, Michael Wiescher

Department of Physics, University of Notre Dame, Notre Dame, IN 46556; hschatz@sulfur.helios.nd.edu, wiescher@nd.edu

ABSTRACT

Hot (explosive) hydrogen burning or the Rapid Proton Capture Process (rp-process) occurs in a number of astrophysical environments. Novae and X-ray bursts are the most prominent ones, but accretion disks around black holes and other sites are candidates as well. The expensive and often multidimensional hydro calculations for such events require an accurate prediction of the thermonuclear energy generation, while avoiding full nucleosynthesis network calculations.

In the present investigation we present an approximation scheme which leads to an accuracy of more than 15 per cent for the energy generation in hot hydrogen burning from 10^8–1.5×10^9 K, which covers the whole range of all presently known astrophysical sites. It is based on the concept of slowly varying hydrogen and helium abundances and assumes a kind of local steady flow by requiring that all reactions entering and leaving a nucleus add up to a zero flux. This scheme can adapt itself automatically and covers situations at low temperatures, characterized by a steady flow of reactions, as well as high temperature regimes where a (p,γ)–(γ,p)-equilibrium is established, while β^+-decays or (α,p)-reactions feed the population of the next isotonic line of nuclei.

In addition to a gain of a factor of 15 in computational speed over a full network calculation, and an energy generation accurate to more than 15 per cent, this scheme also allows to predict correctly individual isotopic abundances. Thus, it delivers all features of a full network at a highly reduced cost and can easily be implemented in hydro calculations.

Subject headings: nuclear reactions, nucleosynthesis, abundances — stars: novae — X-rays: bursts

1. INTRODUCTION

Close binary stellar systems can exchange mass, when at least one of the stars fills its Roche Lobe. After a critical mass ΔM of unburned transferred matter is accumulated on the surface of the accreting star, ignition sets in, typically under degenerate conditions when the accreting object is a white dwarf or neutron star. Degenerate conditions for which the pressure is not a function of temperature, prevent temperature adjustment via pressure increase and expansion and cause a thermonuclear runaway and explosive burning. For white dwarfs, a layer of 10^{-5}–10^{-4} $M_\odot$ forms, before pycnonuclear ignition of hydrogen burning sets in (e.g. Sugimoto & Nomoto 1980; Starrfield et al. 1993; Coc et al. 1995) and causes a nova event (explosive H-burning on white dwarfs) with maximum temperatures of $\approx$(2–3)$\times 10^8$ K and a total energy release of 10^{46}–10^{47} ergs. The burning takes 100–1000 s before the partially burned hydrogen envelope is ejected.

X-ray bursts (for an observational overview see Lewin, van Paradijs, & Taam 1993) involve accreting neutron stars with an unburned, hydrogen-rich surface layer. The critical size of the hydrogen layer before ignition is as small as 10^{-12} $M_\odot$. Temperatures of the order (1-2)$\times 10^9$ K and densities $\rho \approx 10^6$–10^7 g cm^{-3} are attained (see e.g. Wallace & Woosley 1981; Ayasli & Joss 1982; Hanawa, Sugimoto, & Hashimoto 1983; Woosley, Taam, & Weaver 1986; Taam et al. 1993; Taam, Woosley, & Lamb 1996). This explosive burning with rise times of about 1–10 s leads to the release of 10^{39}–10^{40} ergs. Many of the observed features and general characteristics are understood, however, there is still a lack of a quantitative understanding of the detailed observational data. Another aspect is that the explosion energies are smaller than the gravitational binding energy of the accreted hydrogen envelope. An evenly distributed explosion energy would not unbind and eject matter. It remains to be seen whether an interesting amount of matter can escape the neutron star. Super-Eddington X-ray bursts (Taam et al. 1996) are the best candidates for this behavior.

A description of hot (explosive) hydrogen burning has been given by Arnould et al. (1980), Wallace & Woosley (1981), Ayasli & Joss (1982), Hanawa et al. (1983), Wiescher et al. (1986), van Wormer et al. (1994), Thielemann et al. (1994) [see also Biehle (1991), Biehle (1994), Cannon et al. (1992), and Cannon (1993) for Thorne-Zytkow objects, but see the recent results by Fryer, Benz, & Herant (1996) which puts doubts on their existence]. The burning is described by proton captures, β^+-decays, and possibly alpha-induced reactions on unstable proton-rich nuclei, usually referred to as the rp-process (Rapid Proton Capture Process). Cross sections can either be obtained from the best available application of present experimental knowledge, e.g. the determination of resonance properties from mirror nuclei and transfer and/or charge exchange reaction studies, or actual cross section measurements, like for $^{13}\mathrm{N}(p,\gamma)^{14}\mathrm{O}$, the first reaction cross section analysed with a radioactive ion beam facility (see Champagne & Wiescher 1992 and references therein). There exist two major motivations in nuclear astrophysics (a), to understand the reaction flow to a necessary degree, in order to predict the correct energy generation required for hydrodynamic, astrophysical studies, and (b), to predict a detailed isotopic composition which helps to understand the contribution of the process in

question to nucleosynthesis in general. Our main motivation in this paper is (a), to provide a fast energy generation network as a tool for nova and X-ray burst studies. This might be underlined by the fact that novae and X-ray bursts seem not to be major contributors to nucleosynthesis due to the small ejected masses involved or the question whether gravitational binding can be overcome at all. [However, novae can be important for nuclei like ^{7}Li, ^{15}N, ^{22}Na, ^{26}Al, and even Si and S; and super-Eddington X-ray bursts (Taam et al. 1996) will be able to eject some matter, probably containing some light p-process elements.] It will turn out at the end that our efficient approximation and energy generation scheme can also be used to predict abundances accurately. The nucleosynthesis for nuclei above Kr will, however, be discussed in a second paper (Schatz et al. 1996).

In order to understand the energy generation correctly, we have to be able to understand the main reaction fluxes. In the past we performed a series of rp-process studies (Wiescher et al. 1986 to Ar, and van Wormer et al. 1994, extending up to Kr). The reaction rate predictions were based on resonance and direct capture contributions for proton-rich nuclei, making use of the most recent experimental data. Several (p,γ)-reaction rates below mass A=44 have been recalculated by Herndl et al. (1995) in the framework of a shell model description for the level structure of the compound nucleus. A preliminary analysis of the major aspects was given by Thielemann et al. (1994). In the following section 2 we will present this in more detail and discuss the constraints which an approximation scheme has to fulfill in the whole range of temperatures occurring in explosive hydrogen burning environments, i.e. 10^8–1.5×10^9 K. The approximation scheme will be presented in section 3, its application and comparison with full network calculations in section 4, followed by concluding remarks in section 5.

2. REACTION FLOWS IN EXPLOSIVE HYDROGEN BURNING

At low temperatures, the rp-process is dominated by cycles of two successive proton captures, starting out from an even-even nucleus, a β^+-decay, a further proton capture (into an even-Z nucleus), another β^+-decay, and a final (p,α)-reaction close to stability (similar to the hot CNO). The final closing of the cycle via a (p,α)-reaction occurs because proton capture Q-values increase with increasing neutron number N in an isotopic chain for a given Z, while α-capture Q-values or -thresholds show a very weak dependence on N. Thus, a cycle closure occurs at the most proton-rich compound nucleus, which has a lower alpha than proton-threshold. These are the even-Z and especially well bound "alpha"-nuclei with isospin $T_z=(N-Z)/2=0$, like ^{16}O, ^{20}Ne, ^{24}Mg, ^{28}Si, ^{32}S, ^{36}Ar, ^{40}Ca. Therefore, (p,α)-reactions can operate on odd-Z targets with $T_z=+1/2$: ^{15}N, ^{19}F, ^{23}Na, ^{27}Al, ^{31}P, ^{35}Cl, ^{39}K. The hydrogen burning cycles are connected at these nuclei, due to a possible competition between the (p,γ)- and (p,α)-reaction. An exception to the rule is the Ne isotopic chain, where the transition happens already for the compound nucleus ^{19}Ne. Thus, $^{18}\mathrm{F}(p,\alpha)^{15}\mathrm{O}$ is a possible reaction, bypassing the OF(Ne)-cycle. Therefore, only the extended CN(O)-, the NeNa-, MgAl-, SiP-, SCl-cycles etc. exist. This is displayed in Figure 1.

The progress of burning towards heavier nuclei depends on the leakage ratio $(p,\gamma)/(p,\alpha)$

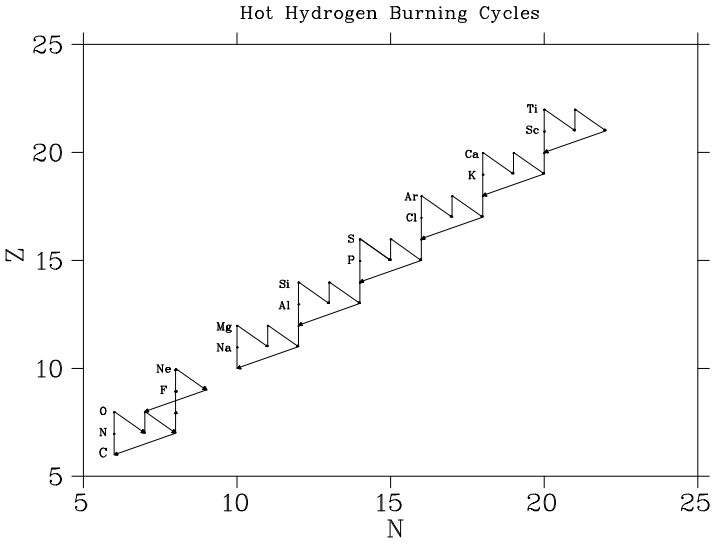

Fig. 1.— The hot hydrogen burning cycles, established at T_9=0.3 and ρ=10^4 g cm $^{-3}$.

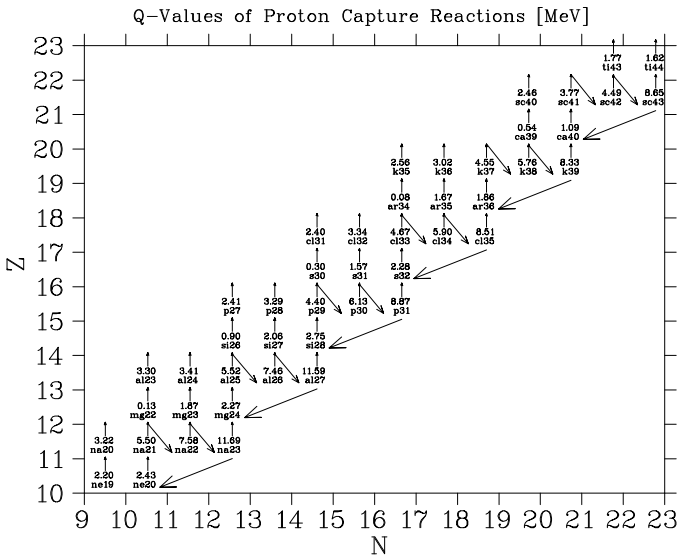

Fig. 2.— Q-values of (p,γ)-reactions between ^{20}Ne and ^{44}Ti.

into the next cycle, which makes a good experimental determination of these reactions important and is possible as we deal here with stable targets. On the other hand, the excitation energies in the corresponding compound nuclei are of the order 8.5–12 MeV and make statistical model approaches also reliable (see e.g. the experiments by Iliadis et al. 1993, 1994 and Ross et al. 1995 for ^{31}P(p,γ), and ^{35}Cl(p,γ) and the later discussion).

Increasing temperatures allow to overcome Coulomb barriers and extend the cycles to more proton-rich nuclei, which permit additional leakage via proton captures, competing with long β-decays. The cycles open first at the last β-decay before the (p,α)-reaction via a competing proton capture, i.e. at the even-Z T_z=–1/2 nuclei like ^{23}Mg, ^{27}Si, ^{31}S, ^{35}Ar, and ^{39}Ca, excluding ^{15}O (because ^{16}F is particle unstable) and ^{19}Ne, which is bypassed by the stronger ^{18}F(p,α)-rate. These nuclei are only one unit away from stability and have small decay Q-values and long half-lives. The situation is illustrated in Figure 2, which shows the possible break-out points and the Q-values of the proton capture reactions. Since the reaction proceeds towards the proton drip-line and into an odd-odd nucleus, the capture Q-values of these (p,γ)-reactions are small (generally less than 2 MeV). This implies a too small density of excited states for employing statistical model cross sections (see discussion in the following paragraphs). At about 3×10^8 K essentially all such cycles are open and a complete rp-pattern of proton captures and β-decays is established, with the exception of the extended CNO-cycle. The process time is determined by the sum of β-decay and proton capture time scales, τ_β and $\tau_{p,\gamma}$, along the rp-path, which does generally not extend more proton-rich than T_z=–1 for even-Z nuclei. The reaction time scales are dominated by the T_z=–1/2 even-Z nuclei close to stability, listed above.

At 4×10^8 K the CNO-cycle breaks open via ^{15}O$(\alpha,\gamma)^{19}$Ne. ^{14}O$(\alpha,p)^{17}$F can also lead to a successful break-out when followed by a proton capture and (α,p)-reaction on ^{18}Ne.

Due to higher energies, Coulomb barriers can be more easily overcome by heavier projectiles (like alpha captures on CNO-targets), and proton captures can occur further away from stability. However, in all cases the decay of T_z=–1 even-Z nuclei (and at high densities the competition with (α, p)-reactions) is a prominent part of the reaction path. Alpha-reactions are not important for Z>20, due to increasing Coulomb barriers and decreasing Q-values. For heavier nuclei beyond Ca, the reaction pattern seems complicated. However, temperatures approaching 10^9 K cause strong photodisintegrations for proton capture Q-values smaller than $25kT \approx 3$ MeV, which is comparable to Q-values found for even-Z T_z=–1 nuclei. [25-30$kT \geq Q$ is a rough criterion to find out whether photodisintegrations can counterbalance capture reactions and lead to an equilibrium situation.] Thus, reactions breaking out of the cycles discussed above (up to the proton drip line) come into a (p, γ)–(γ, p)-equilibrium along isotonic lines with equal N. Under such circumstances the nuclear connection boils down to the necessary knowledge of nuclear masses and β-decay half-lives, similar to the r-process experiencing an (n, γ)–(γ, n)-equilibrium in isotopic chains (see Cowan, Thielemann, & Truran 1991; Kratz et al. 1993; Meyer 1994).

The general situation is explained in Figure 3, which contains all possible reactions from the original cycles over proton captures breaking out of the cycles, the accompanying beta decays and (α, p)-reactions bridging waiting points with long decay half-lives. By comparing with Figure 2, which also lists the Q-values involved, Figures 4a and 4b give an indication for the minimum temperatures required to permit statistical model calculations for proton and alpha-induced reactions. The

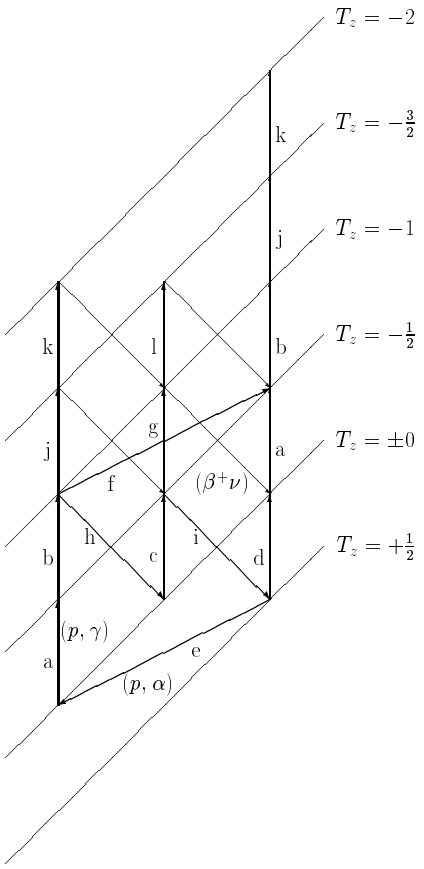

Fig. 3.— Recurrent structure in the rp-process network.

reason is that a high density of compound nuclear states is necessary for statistical model calculations to become reliable. The energy of the Gamow peak, where the integrand in a thermonuclear cross section integral (cross section times Boltzmann distribution) has a maximum, increases with increasing temperature. Because higher level densities are encountered at higher excitation energies corresponding to higher temperatures of the Boltzmann distribution, a critical temperature exists beyond which such calculations are reliable (for more details see Rauscher, Thielemann, & Kratz 1996). We can analyse the expected behavior: Reactions j, k, and l of Figure 3 have reaction Q-values less than $\approx$3 MeV and for conditions close to 10^9 K we have $25kT \approx Q$ which permits a (p, γ)–(γ, p)-equilibrium. Thus, although the cross sections are highly uncertain and statistical model approaches are not valid (see Figure

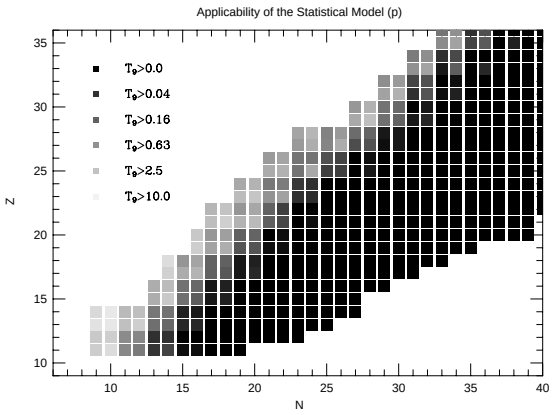

Fig. 4a.— Applicability of the Statistical Model for (p,γ)- and (p,α)-reactions.

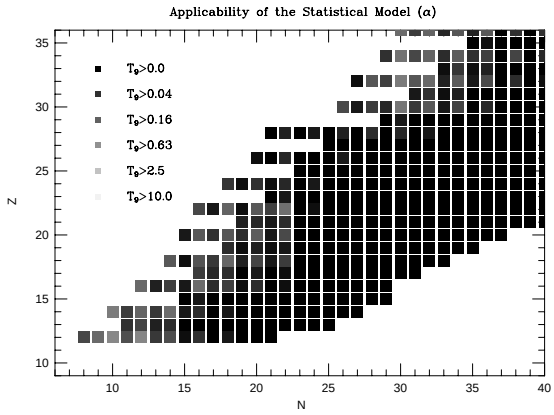

Fig. 4b.— Applicability of the Statistical Model for (α,γ)- and (α,p)-reactions.

4a), only the Q-values, i.e. masses, are needed for these nuclei. Reactions b, c, d, and e [(p,γ) and (p,α) reactions] have Q-values in excess of 5 MeV and in most cases high enough level densities to ensure the usage of statistical model cross sections for the appropriate temperature regime. Reaction f, an (α,p)-reaction, provides also a sufficiently high level density to apply statistical model cross sections (see Figure 4b, for ^{18}Ne(α,p) see Görres & Wiescher 1995). Reaction g is crucial for the break-out, a statistical model approach is clearly not permitted, and a (p,γ)–(γ,p)-equilibrium is not valid at the lower appropriate temperatures of about 3-4$\times10^8$ K. Thus, all reactions of type g ask strongly for experimental determination, possibly with radioactive ion beams. Reactions h, i and all other connecting β-decays are required, preferably from experiments, otherwise from theoretical QRPA predictions.

Beyond Ca and Ti, this scheme simplifies into one dominated by proton captures and beta-decays, with the proton captures in a (p,γ)–(γ,p)-equilibrium. The proton drip line develops a zig-zag shape and can separate two even-Z proton-stable nuclei on the same isotone by an unstable odd-Z nucleus. Görres et al. (1995) have shown that such gaps can be bridged by two-proton capture reactions, proceeding through the unstable nucleus, similar to the 3α-reaction passing through ^{8}Be. This can extend the (p,γ)–(γ,p)-equilibrium beyond the drip line to proton-stable "peninsulas", thus avoiding long beta-decay half-lives. While alpha-induced reactions are not important for nuclei beyond Ca and Ti, small Q-values for $A > 56$ can permit (γ,α)-photodisintegrations and cause a back flow, decreasing the build-up of heavy nuclei.

After having analized the reaction patterns in the previous discussion, we have now to implement these findings into an approximation which can handle and describe all of the patterns. Considering the hydrogen and helium abundances as slowly varying, and assuming a kind of local steady flow by requiring that all reactions entering and leaving a

nucleus add up to a zero flux, we will devise a scheme which can adapt itself to the whole range of conditions of interest in hot hydrogen burning. It can automatically cover situations at low temperatures, characterized by a steady flow through all connected hot CNO-type cycles and branchings feeding the next cycle, to high temperature regimes where a (p,γ)–(γ,p)-equilibrium is established, while β-decays or (α,p)-reactions feed the population of the next isotonic line. The details are discussed in the following section.

3. APPROXIMATION SCHEME

3.1. Reaction Rates and Quasi-Decay Constants

The thermonuclear reaction rates used in our calculations have been discussed in detail by van Wormer et al. (1994) (*cf.* the appendix therein).[1] The temporal change of the isotopic abundances $Y_i{=}\frac{X_i}{A_i}$ can be calculated by all depleting and producing reactions

$$Y_i = \sum_j {}^i\alpha_j\, Y_j + \sum_{j,k} {}^i\alpha_{j,k}\, Y_j\, Y_k + \sum_{j,k,l} {}^i\alpha_{j,k,l} Y_j\, Y_k\, Y_l\,. \qquad (1)$$

The first term in (1) includes all one-particle reactions (decays or photodisintegrations) of nuclei j producing ($i{\neq}j$) or destroying ($i{=}j$) nucleus i. The α_j are either decay constants or effective temperature dependent decay constants in the case of photodisintegrations. The second sum represents all two-particle reactions between nuclei j,k with

[1]The parameterized reaction rates can be found for instance in the database REACLIB located at http://csa5.lbl.gov/~fchu/astro.html/.

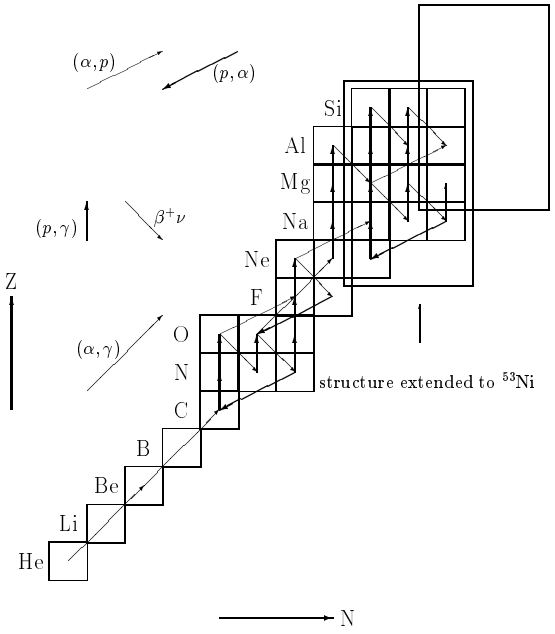

Fig. 5a.— rp-process network being used in the approximation. The structure in the box is eight times repeated up to ^{50}Mn. Bold arrows correspond to large, normal arrows to small decay constants.

${}^i\alpha_{j,k}{=}{}^ic_{j,k}\,\rho N_A{}^i\langle\sigma v\rangle_{j,k}$. Similarly, the third term represents three particle processes with ${}^i\alpha_{j,k}\,{=}{}^ic_{j,k,l}\rho^2N_A^{2\,i}\langle\sigma v\rangle_{j,k,l}$ (Fowler, Caughlan, & Zimmermann 1967). The coefficients c include the statistical factors for avoiding double counting of reactions of identical particles.

van Wormer et al. (1994) investigated numerically which reactions must be considered in the rp-process. Apart from the temperature insensitive β^+-decays, the only one-particle reactions which must be especially considered at high temperatures are photodisintegrations. The two-body reactions dominating the rp-process are (p,γ)-, (p,α)- and, (α,p)-reactions. Three body reactions can be neglected in explosive hydrogen burning with the exception of the 3α-reaction which plays a central role in this context. Taking into account individual reactions, equation (1) can

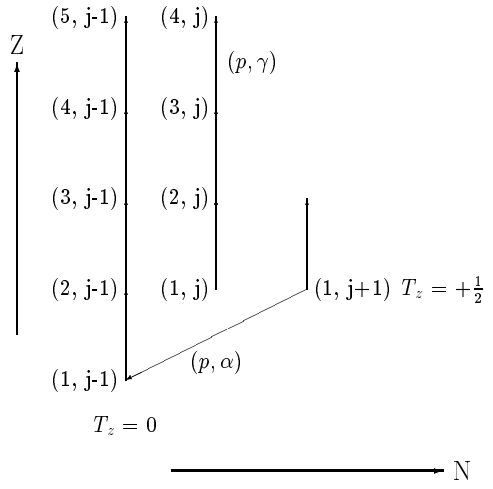

Fig. 5b.— The proton capture sequences are connected to each other by (α, p)- and (β^+, ν)-breakout reactions respectively.

be rewritten as

$$\begin{aligned}\dot{Y}_i &= \sum_j {}^i\lambda_j^{\beta^+} Y_j + \sum_j {}^i\lambda_j^{\gamma,p} Y_j \\ &\quad + \sum_j \rho N_A {}^i\langle\sigma v\rangle_{j,p} Y_j Y_p \\ &\quad + \sum_j \rho N_A {}^i\langle\sigma v\rangle_{j,\alpha} Y_j Y_\alpha \,. \end{aligned} \tag{2}$$

If the proton and helium abundances do not change greatly during relevant rp-process time scales, we are able to describe proton captures and (α, p)-reactions with *quasi-decay constants*, provided that temperature and density do not change greatly during the process time scale of interest:

$$\begin{aligned} {}^i\lambda_j^{p,\gamma} &:= \rho N_A {}^i\langle\sigma v\rangle_{j,p} Y_p = \text{const} && \text{(3a)} \\ {}^i\lambda_j^{p,\alpha} &:= \rho N_A {}^i\langle\sigma v\rangle_{j,p} Y_p = \text{const} && \text{(3b)} \\ {}^i\lambda_j^{\alpha,\gamma} &:= \rho N_A {}^i\langle\sigma v\rangle_{j,\alpha} Y_\alpha = \text{const} && \text{(3c)} \\ {}^i\lambda_j^{\alpha,p} &:= \rho N_A {}^i\langle\sigma v\rangle_{j,\alpha} Y_\alpha = \text{const}\,. && \text{(3d)} \end{aligned}$$

Thus the system of nonlinear differential equations can be written in a linearized form

$$\dot{Y}_i = \sum_j {}^i\lambda_j^x Y_j \,, \tag{4}$$

where x represents one of the following reactions: (γ, p), (p, γ), (α, p), (p, α), (α, γ), (γ, α), $(\beta^+\nu)$. When we choose $\mathrm{Y_0}$=($Y_1, \ldots, Y_i, \ldots, Y_n$) to represent the initial abundance distribution, the system of equations (4) can be written as

$$\dot{\mathrm{Y}} = A\,\mathrm{Y}\,, \quad A\,(N \times N)\text{-matrix}\,. \tag{5}$$

Such systems of linear differential equations with *constant* coefficients can be solved by Jordan-normalizing matrix A. Its transformation

$$J = SAS^{-1}\,,\ S\,\epsilon\,\mathrm{GL_n}(\mathbb{R}) \tag{6}$$

yields the N-dimensional set of eigenfunctions

$$u_{i;j}(t) = e^{\lambda_i^m t} p_{i;j}(t)\,. \tag{7}$$

Here, λ_i^m represents eigenvalue i with degeneracy m, $u_{i;j}$ eigenvector j to eigenvalue i ($1 \leq j \leq m$) and $p_{i;j}(t)$ a polynomial of degree (j–1). However, the transformations $u'_{i;j} = S\,u_{i;j}$ are in general difficult to survey and to handle. Furthermore, the elements of A become slowly varying functions when the abundances of hydrogen and helium change slightly over a certain process time scale. This is for instance the case, when we consider hot hydrogen burning. Only numeric simulations will be feasible for these two reasons.

We will show in the following subsection how certain sequences of a thermonuclear reaction network can be regarded as *quasi-*

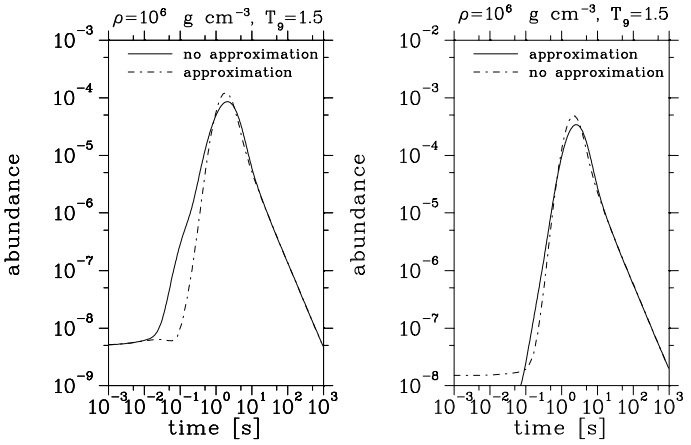

Fig. 6a.— Comparison of the approximated abundances of ^{53}Ni and ^{55}Ni with results from full network calculations.

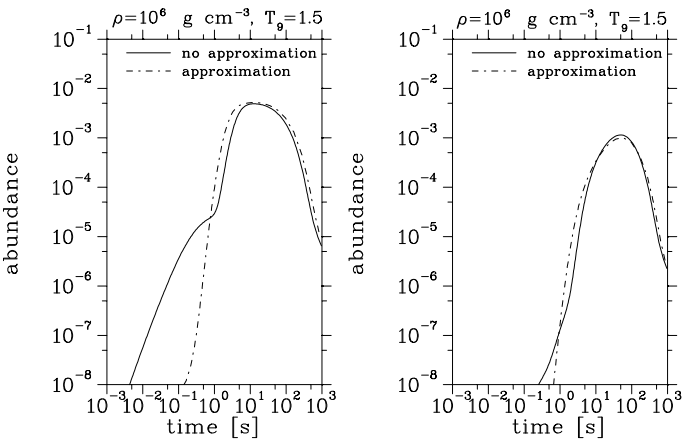

Fig. 6b.— Same as Figure 6a but for ^{64}Ge and ^{72}Kr.

nuclei. In such sequences a steady flow materializes and the ratios between the different abundances are constant and are only determined by the values of the quasi-decay constants. A procedure of this kind provides us with a system of equations with a smaller dimension, which can be solved numerically.

3.2. The Approximation

In section 2, we discussed the burning cycles with the same structure as the hot CNO-cycle (see also Figures 1–3). It is well understood how a steady state equilibrium is established in hot CNO-like reaction chains at temperatures $T_9 \simeq 0.2$ and on time scales governed by the longest β^+-decay in the cycle. Then the abundance $Y_{i,j}$ of nucleus (i) in a cycle (j) can be calculated from the equilibrium condition

$$\dot{Y}_{i,j} \stackrel{!}{=} 0. \qquad (8)$$

This condition can be used for simplifying the system of equations which determines the thermonuclear reaction flows. However, an approximation of this kind is no longer justified, when we consider time scales shorter than the half-lives of the β^+-unstable nuclei or temperatures greater than T_9=1 where photodisintegrations become so important that a (p,γ)–(γ,p)-equilibrium is attained rather than a steady flow (see Figure 3). Then, proton-induced reactions can be associated with large quasi-decay constants and, in comparison to β-decays, small half-lives. Thus, all the abundances of isotonic nuclei which are connected by proton capture reactions can be considered in a quasistatic equilibrium on time scales exceeding the half-lives associated with the quasi-decay constants. Such sequences shall be now defined as quasi-nuclei.

In the following paragraphs, the abundances of nuclei in proton capture sequences shall be calculated under the assumption of a quasistatic equilibrium. Consider the j^{th} of m sequences which consists of $n-1$ proton captures between n nuclei (*cf.* Figure 5b: Here, two proton capture sequences are shown with n=4 and n=5). Each nucleus (i) in a sequence (j) is involved in $k+2$ reactions including proton captures and photodisintegrations. Furthermore, we assume for simplicity that the

abundances of helium and hydrogen stay constant over the time scale of interest and that nucleus (i,j) is not fed by reactions from another chain j'. Using the equilibrium condition (8), the temporal change of the abundance of a nucleus (i,j) can be written as

$$\begin{aligned}\dot{Y}_{i,j} &= \lambda^{p,\gamma}_{i-1,j} Y_{i-1,j} - \sum_k \lambda^{x}_{i,j,k} Y_{i,j} \\ &\quad + \lambda^{\gamma,p}_{i+1,j} Y_{i+1,j} = 0 \ . \end{aligned} \tag{9}$$

The terms summed over k are leaks out of chain (j) via nucleus (i,j) The extreme cases of flux equilibria, like steady flows on the one hand ($\lambda^{p,\gamma} \gg \lambda^{\gamma,p}$, λ^{β^+}) and (p,γ)–(γ,p)-equilibria on the other hand ($\lambda^{p,\gamma}$, $\lambda^{\gamma,p} \gg \lambda^{\beta^+}$) can be discussed on the basis of this equation. Here, the general case shall be discussed.

For a chain of n nuclei, $n-1$ such equations permit to relate the abundance $Y_{i-1,j}$ to $Y_{i,j}$ starting with a "known" $Y_{n,j}$, the abundance of the last nucleus in a sequence. Thus we obtain for each sequence (j) an $(n-1)$-dimensional system of linear equations which allows us to express each abundance $Y_{i,j}$ in terms of $Y_{n,j}$:

$$Y_{i,j} = v_{i,j}(\lambda^{x}_{1,j} \ldots \lambda^{x}_{n,j}) Y_{n,j} \ . \tag{10}$$

The $v_{i,j}$ depend only on the constant or slowly varying quasi-decay constants $\lambda_{i,j}$. The abundance of a sequence can be treated as the abundance of a quasi-nucleus by $Y_j := \sum_i Y_{i,j}$. When Y_j is already determined at a point in time $t=t_s$, each abundance $Y_{i,j}$ can be written as

$$Y_{i,j}(t_s) = \frac{v_{i,j}}{v_j} Y_j(t_s) \ , \tag{11}$$

with $v_j = \sum_i v_{i,j}$. Hence, when the abundances of the quasi-nuclei Y_j are given at a time t,

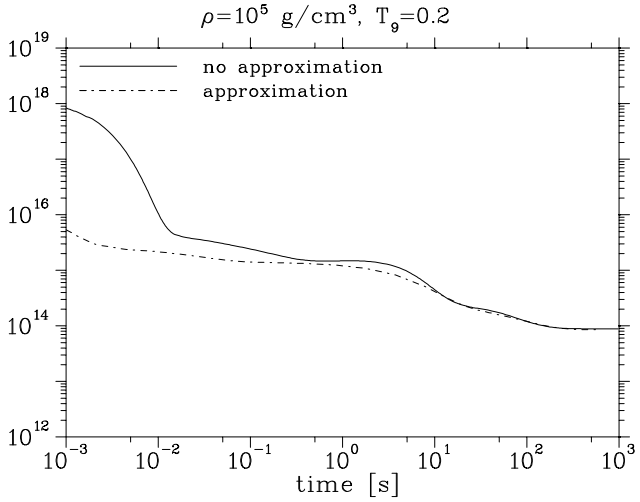

Fig. 7a.— Comparison of the energy generation rate $\dot{\epsilon}$ for for nova-like conditions.

the abundances $Y_{i,j}(t)$ in each sequence can be determined *simultaneously*.

However, we also have to take care of incoming fluxes into a sequence (j) not jet considered in equation (9). As a consequence, the coefficients $v_{i,j}$ are no longer constant because they become explicitly abundance-dependent for the following reason: in contrast to the *outgoing* fluxes, the *incoming* fluxes into a sequence j are *not* proportional to the abundances $Y_{i,j}$ of the nuclei in this sequence. Therefore, abundances can no longer be determined simultaneously.

Incoming fluxes can nevertheless be considered as long as the abundances do not change too fast during a time step. We can add to equation (9) all incoming fluxes from nuclei (l) of different chains (m) proportional to their abundances $Y_{l,m}(t_{s-1})$, $m \neq$ j (when no time t is indicated, the quantities are given at $t=t_s$),

$$\dot{Y}_{i,j} = -Y_{i,j} \sum_k \lambda^{x}_{i,j,k} + \lambda^{\gamma,p}_{i+1} Y_{i+1,j} + \lambda^{p,\gamma}_{i-1,j} Y_{i-1,j}$$

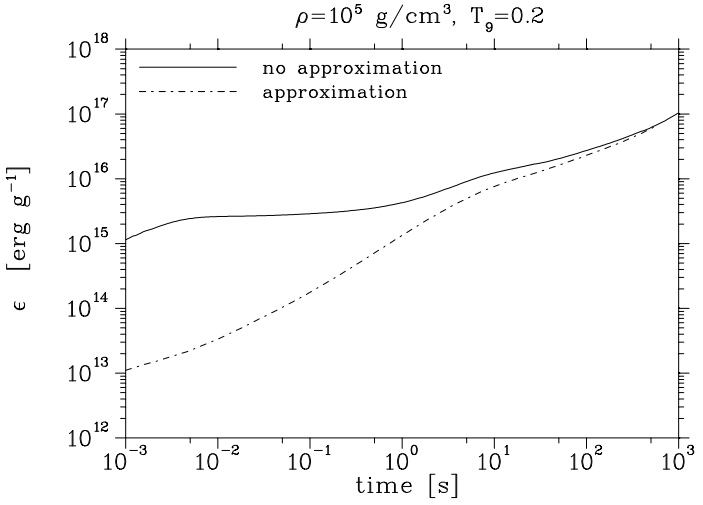

Fig. 7b.— Comparison of the energy generation ϵ for nova-like conditions.

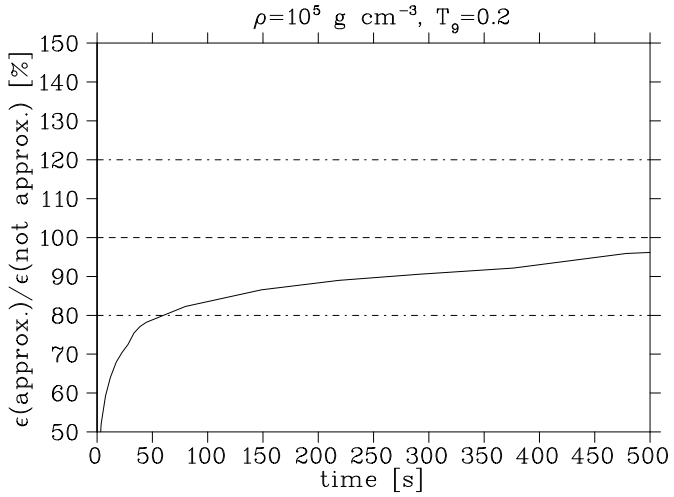

Fig. 7c.— With this approximation, energy generation for nova-like conditions can be reproduced with an accuracy of 15-5 per cent.

$$+ \sum_{\substack{l,m \\ m\neq j}} \lambda^x_{l,m} Y_{l,m}(t_{s-1}) = 0 \; . \qquad (12)$$

This can be solved for $Y_{i-1,j}$, leading to

$$Y_{i-1,j} \;=\; \underbrace{\frac{1}{\lambda^{p,\gamma}_{i-1,j}} \left(Y_{i,j} \sum_k \lambda^x_{i,j,k} - \lambda^{\gamma,p}_{i+1} Y_{i+1,j} \right)}_{v_{i-1,j}\, Y_{n,j}}$$

$$- \underbrace{\frac{1}{\lambda^{p,\gamma}_{i-1,j}} \sum_{\substack{l,m \\ m\neq j}} \lambda^x_{l,m} Y_{l,m}(t_{s-1})}_{w_{i-1,j}(\lambda^x_{l,m}, Y_{l,m}(t_{s-1}))} \, , \qquad (13)$$

or more generally

$$Y_{i,j} = v_{i,j}\, Y_{n,j} - w_{i,j}(t_{s-1}) \, . \qquad (14)$$

When a slowly varying function $v'_j(t_{s-1})$ is given so that we can approximate $Y_{n,j}$ by

$$Y_{n,j}(t_s) \approx \frac{1}{v'_j(t_{s-1})} Y_j(t_s) \; , \qquad (15)$$

we can extend $w_{i,j}$ in (14) as follows

$$Y_{i,j} = v_{i,j} Y_{n,j} - \frac{v'_j}{Y_j} w_{i,j} Y_{n,j} \, , \qquad (16)$$

and finally obtain

$$Y_{i,j} = v'_{i,j} Y_{n,j} \qquad (17)$$

$$v'_{i,j} = v_{i,j} - \frac{v'_j}{Y_j} w_{i,j} \, , \qquad (18)$$

with v'_j=$\sum_i v'_{i,j}$. Setting $v'_{i,j}(t_0$=$0)$=$v_{i,j}(t_0$=$0)$ as initial values, the existence of the functions v'_j is guaranteed.

So far we have made two approximations. (a): including reactions within a chain and leaks out of a chain described by equation (9). In that case all abundances could be described simultaneously. (b): When also considering incoming fluxes [see equation (12)], we become dependent on abundances in other chains. Approximating their abundances at t=t_s by abundances at t'=t_{s-1} permits to stay within the same approximation scheme. But we have to be aware that this is only valid

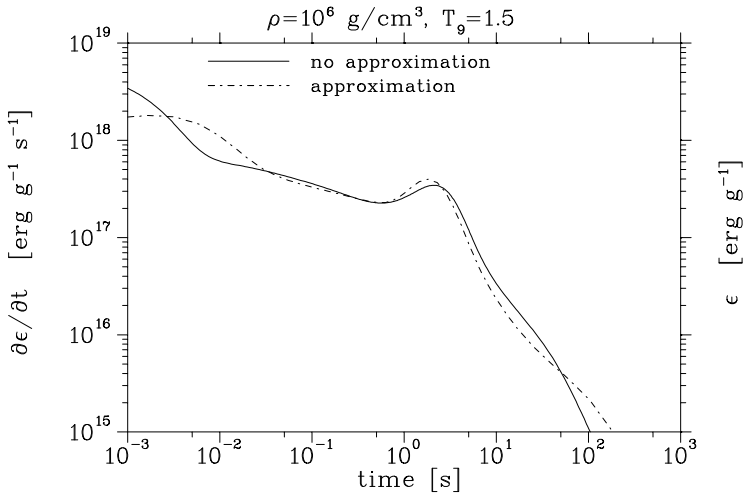

Fig. 8a.— Same as Figure 7a but for X-ray burst conditions.

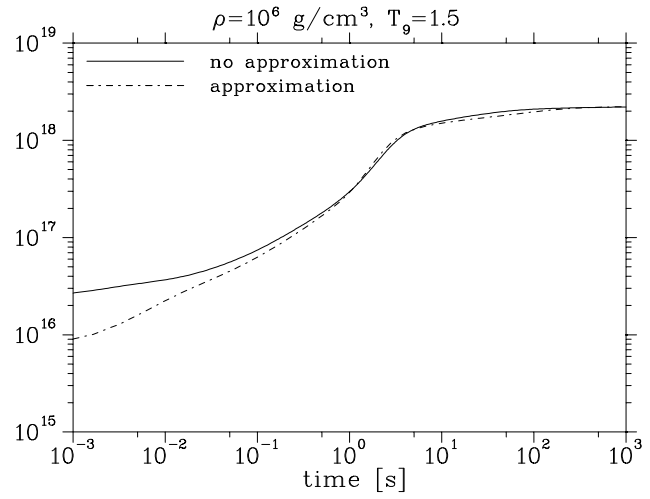

Fig. 8b.— Same as Figure 7b but for X-ray burst conditions.

for slowly varying abundances or equivalently small time steps.

We obtained this approximation under the assumption that the abundances of hydrogen and helium stay constant. Y_p and Y_α are slowly varying functions in realistic environments. We can adjust for the change of Y_p and Y_α and obtain their new values applying relation (11)

$$\dot{Y}_p = \sum_{i,j}(\lambda_{i,j}^{\gamma,p} + \lambda_{i,j}^{\alpha,p} - \lambda_{i,j}^{p,\alpha} - \lambda_{i,j}^{p,\gamma})Y_{i,j}(t_s) \quad (19a)$$

$$\dot{Y}_\alpha = \sum_{i,j}(\lambda_{i,j}^{p,\alpha} - \lambda_{i,j}^{\alpha,p} + \lambda_{i,j}^{\gamma,\alpha} - \lambda_{i,j}^{\alpha,\gamma})Y_{i,j} \; . \quad (19b)$$

As a consequence, the quasi-decay constants must be recalculated after each time step, making use of the updated proton and alpha abundances considering them constant for one time step.

Thus it is possible to express simultaneously every abundance $Y_{i,j}$ in a sequence with the sequence abundance Y_j. With an approximation scheme of this kind, we reduced our full network described by $\sum_{j=1}^{m} n(j)$ equations to a system of m equations. In the following we want to check the accuracy of such an approximation.

4. RESULTS

The calculations were done with a reaction network which consists mainly of proton capture sequences, each starting out from a T_z=0 nucleus. The number of nuclei in a sequence is determined by the condition that the quasi decay constant ${}^{i+1}\lambda_i^{p,\gamma}$ of a nucleus (i) into nucleus (i+1) is larger than a certain $\lambda_{\rm min}$. When this condition is fulfilled, nucleus (i+1) is considered to be in the sequence. For the following calculations $\lambda_{\rm min}$ was set to 10^3 s^{-1} because we wanted to reproduce the energy generation of explosive hydrogen burning on time scales τ=$\lambda_{\rm min}^{-1} > 10^{-2} - 10^{-1}$ s. As a consequence, a sequence contains not more than 5 nuclei for temperatures $T_9 \leq 1.5$ and densities $\rho \leq 10^6$ g cm^{-3}.

In addition to the proton capture sequences,

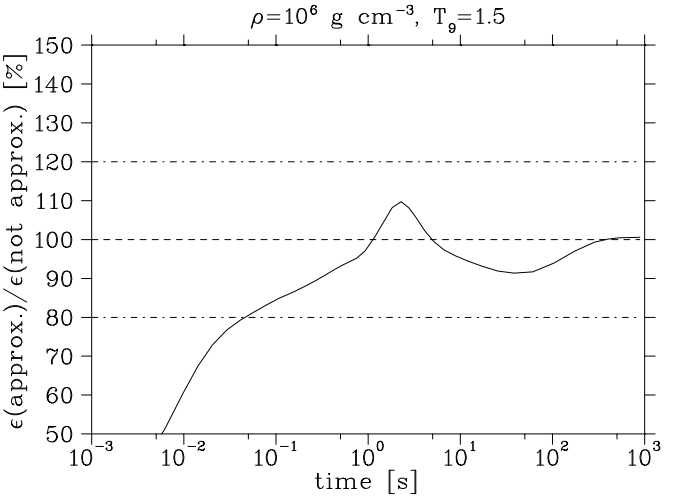

Fig. 8c.— Same as Figure 7c but for X-ray burst conditions.

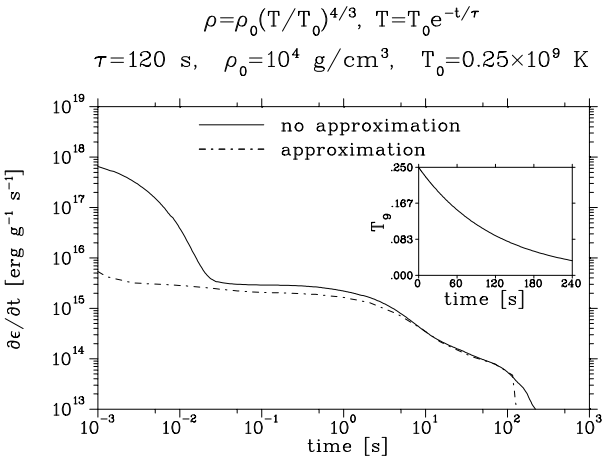

Fig. 9.— Same as Figure 7a but for varying density and temperature starting with novae peak conditions. The approximation is valid as long as the temperature does not fall considerably below $T_9 = 0.1$.

T_z=$\frac{1}{2}$ nuclei had to be considered in the network. They are the most neutron-rich nuclei of the hot CNO-type cycles, where after a proton capture, the alpha-threshold in the compound nucleus is lower than the proton-threshold, and (p, α)-reactions can occur which compete with the still possible (p, γ)-transitions (see Figure 5b). Since the (p, α)- and (p, γ)-reactions occur on the same time scale, these T_z=$\frac{1}{2}$ nuclei can not affiliated to a proton capture chain but have to be considered separately.

Between ^{12}C and ^{50}Mn, the network can be composed of proton capture reaction sequences and T_z=$\frac{1}{2}$ nuclei with one exception. The transition occurs already at compound nucleus ^{19}Ne in the Ne isotopic chain. A (p, α)-reaction is possible on the T_z=0 nucleus ^{18}F and a proton capture reaction sequence starts out from ^{19}Ne with isospin T_z=$-\frac{1}{2}$.

The low alpha-threshold of ^{19}Ne, which caused an exception of the rule and prevented an OFNe-cycle, permits on the other hand the ^{15}O(α, γ)-reaction and triggers the break-out from the CNO-cycles. The network described so far is shown in the Figure 5a and 5b.

At temperatures exceeding T_9=0.8 and $\rho \geq 10^6$ g cm^{-3}, the network must be completed with the 3α-reaction. Furthermore, it is very likely that fluxes up to ^{72}Kr may influence the energy generation. In the region between ^{51}Mn and ^{72}Kr, the β^+-reactions of the for the rp-process relevant nuclei are, with the exception of ^{55}Ni, ^{64}Ge and ^{72}Kr, considerably smaller than the typical time scales of novae and X-ray bursts. Consequently, only the above mentioned nuclei were considered explicitly in the approximation scheme. The approximated abundances of ^{53}Ni and these three waiting point nuclei are compared with full network calculation results in Figure 6a and 6b.

The nuclei used in the approximation scheme are listed in Table 1 according to their affiliation to a certain proton capture reaction chain. Nuclei which had to be considered separately (p, ^{4}He, T_z=$\frac{1}{2}$ nuclei, ^{55}Ni, ^{64}Ge and ^{72}Kr) are given an own sequence number.

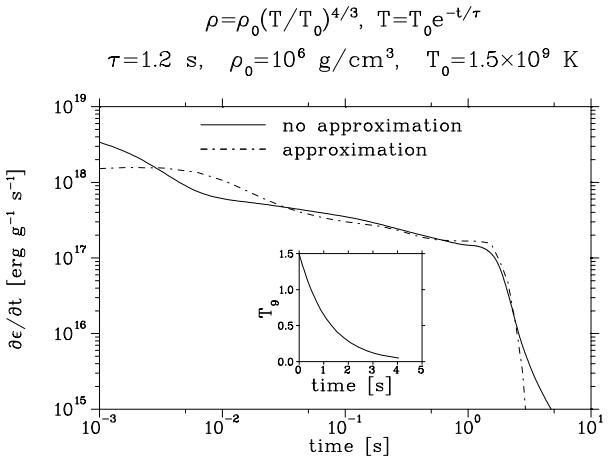

Fig. 10.— Same as Figure 9 but for X-ray burst peak condition.

The waiting point abundances obtained with this approximation are compared with full network calculation results in Figure 6a and 6b.

Approximating the network according to section 3.2, we calculated the energy generation rate $\dot{\epsilon}$ and the integrated energy generation ϵ for nova-like conditions (T_9=0.2, ρ=10^5 g cm^{-3}) and X-ray burst peak conditions (T_9=1.5, ρ=10^6 g cm^{-3}) and compared the results to full size network calculations which take into account each nucleus separately. In each case we assumed a solar abundance distribution for the accreted matter. The results for small temperatures are shown in Figure 7a–7c and those for X-ray burst conditions in Figure 8a–8c. Considering the time scales important for novae (100–1000 s) and X-ray bursts (1–10 s), we see that the approximation scheme devised in section 3 agrees always to a high degree for the astrophysical applications considered here. The overall results show only deviations smaller than 15 per cent or even less (down to 5 per cent) at a gain in computational speed by a factor of 15. Several calculations at intermediate temperatures and densities, i. e. $10^4 \leq \rho \leq 10^6$, $0.2 \leq T_9 \leq 1.5$ confirmed the above mentioned efficiency and accuracy of the approximation scheme.

Such an approximation would not be very useful if it was only valid for constant temperatures and densities. In order to check its accuracy for varying temperatures and densities we assumed after peak conditions were obtained in the ignition an exponentially decreasing temperature and an adiabatically expanding accretion layer with a radiation dominated equation of state ($\gamma = \frac{4}{3}$):

$$T = T_0 e^{-\frac{t}{\tau}} \qquad (20a)$$

$$\rho = \rho_0 \left(\frac{T}{T_0}\right)^{\frac{4}{3}}. \qquad (20b)$$

Using typical peak temperatures T_0, densities ρ_0 and time scales τ for X-ray bursts and novae, we again calculated the energy generation (Figure 9 and 10). The results show that the approximation is valid for changing temperatures and densities as long as they are in the range of $10^4 \leq \rho \leq 10^6$, $0.1 \leq T_9 \leq 1.5$. No significant change in computational speed was observed.

The differences at time scales smaller than t=10^{-2} s are due to the very fast reaction flows within the proton capture reaction chains: They occur in full scale network calculations until equilibrium is reached according to equation (8).

TABLE 1:
PROTON CAPTURE SEQUENCES[1]

Sequence Number	Nuclei
Sequence 1	p
Sequence 2	^{4}He
Sequence 3	^{12}C
	^{13}N
	^{14}O
Sequence 4	^{14}N
	^{15}O
Sequence 5	^{15}N
Sequence 6	^{19}Ne
	^{20}Na
	^{21}Mg
Sequence 7	^{16}O
	^{17}F
	^{18}Ne
Sequence 8	^{20}Ne
	^{21}Na
	^{22}Mg
	^{23}Al
	^{24}Si
Sequence 9	^{22}Na
	^{23}Mg
	^{24}Al
	^{25}Si
Sequence 10	^{23}Na
Sequence 11	^{24}Mg
	^{25}Al
	^{26}Si
	^{27}P
	^{28}S
Sequence 12	^{26}Al
	^{27}Si
	^{28}P
	^{29}S
Sequence 13	^{27}Al
Sequence 14	^{28}Si
	^{29}P
	^{30}S
	^{31}Cl
	^{32}Ar
Sequence 15	^{30}P
	^{31}S
	^{32}Cl
	^{33}Ar
Sequence 16	^{31}P

TABLE 1 — *Continued*

TABLE 1 — *Continued*

Sequence Number	Nuclei
Sequence 17	^{32}S
	^{33}Cl
	^{34}Ar
	^{35}K
	^{36}Ca
Sequence 18	^{34}Cl
	^{35}Ar
	^{36}K
	^{37}Ca
Sequence 19	^{35}Cl
Sequence 20	^{36}Ar
	^{37}K
	^{38}Ca
	^{39}Sc
	^{40}Ti
Sequence 21	^{38}K
	^{39}Ca
	^{40}Sc
	^{41}Ti
Sequence 22	^{39}K
Sequence 23	^{40}Ca
	^{41}Sc
	^{42}Ti
	^{43}V
	^{44}Cr
Sequence 24	^{42}Sc
	^{43}Ti
	^{44}V
	^{45}Cr
Sequence 25	^{43}Sc
Sequence 26	^{44}Ti
	^{45}V
	^{46}Cr
	^{47}Mn
	^{48}Fe

TABLE 1 — *Continued*

Sequence Number	Nuclei
Sequence 27	^{46}V
	^{47}Cr
	^{48}Mn
	^{49}Fe
Sequence 28	^{47}V
Sequence 29	^{48}Cr
	^{49}Mn
	^{50}Fe
	^{51}Co
	^{52}Ni
Sequence 30	^{50}Mn
	^{51}Fe
	^{52}Co
	^{53}Ni
Sequence 31	^{51}Mn
Sequence 32	^{55}Ni
Sequence 33	^{64}Ge
Sequence 34	^{72}Kr

[1]The nuclei used in the approximation scheme are listed according to their affiliation to a certain proton capture reaction chain. Nuclei which had to be considered separately (p, ^{4}He, T_z=$\frac{1}{2}$ nuclei, ^{55}Ni, ^{64}Ge and ^{72}Kr) are given an own sequence number.

5. CONCLUSION

The main motivation for the present investigation was to find a fast and efficient approximation scheme which permits to predict the energy generation in explosive hydrogen burning for a large range of conditions, i.e. temperatures ($0.2 \leq T_9 \leq 1.5$) and densities (10^4 g cm$^{-3} \leq \rho \leq 10^6$ g cm^{-3}) respectively, for applications in hydro calculations which cannot afford full nuclear network. This goal has been achieved. The energy generation of full network calculations (150 nuclei) could be reproduced with a high accuracy, resulting in

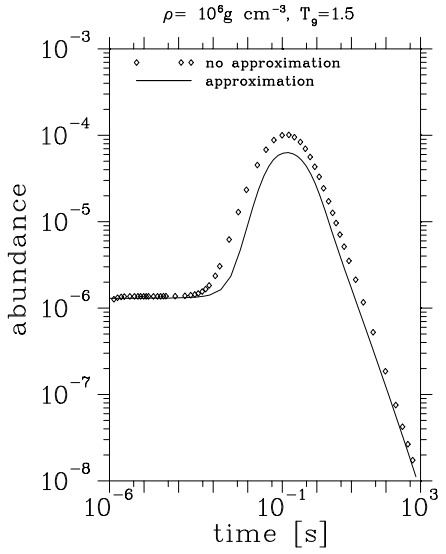

Fig. 11.— Comparison of the ^{33}Ar-abundances calculated by a full network calculation and the approximation scheme.

deviations of 5 to a maximum of 15 per cent while gaining a factor of about 15 in computational speed.

The approximation scheme discussed in this paper is therefore well suited for realistic hydro calculations of novae or X-ray bursts and other possible sites of explosive hydrogen burning.

The additional advantage of this method is that it also permits to predict isotopic abundances with a similar accuracy and can thus even replace full network calculations for this purpose (see Figure 11).

We were also able to determine key nuclear properties, which directly enter the precision of calculations for explosive hydrogen burning, its energy generation and abundance determination. We have identified the even-Z T$_z$=–1/2 nuclei like ^{23}Mg, ^{27}Si, ^{31}S, ^{35}Ar and ^{39}Ca, as essential targets for proton captures which are in competition with β-decays. As their small reaction Q-values (less than 2 MeV) do not permit the application of statistical model cross sections, they have to be determined experimentally. Thus, these results are an ideal guidance for future experimental investigations with radioactive ion beams. Nuclei closer to stability permit the application of statistical model cross sections. Nuclei more proton-rich than T_z=-1 are only populated for conditions when a (p,γ)–(γ,p)-equilibrium is established.

Thus, only their masses, spins and half-lives enter the calculation. Connecting (α,p)-reactions have high enough Q-values, even close to the drip-line, that the level densities are sufficient for statistical model cross sections (this is true at least up to Ca and Ti, where alpha-induced reactions can play an important role). Therefore, the remaining experimental properties which should be determined and enter the calculations in a crucial way are β^+-decay half-lives and nuclear masses. The latter control the abundances in a (p,γ)–(γ,p)-equilibrium. Beyond Se, the details of the proton drip-line are actually not that well known yet, but can influence the endpoint of the rp-process. First calculations which include 2p-capture reactions (Schatz et al. 1996) indicate that it seems possible to produce nuclei with A=90-100 in the rp-process under X-ray burst conditions, depending on the choice of mass formulae and half-life predictions (similar to r-process studies). Especially a region of strong deformation and small α-capture Q-values around A=80 seems to be predicted with large variations among different mass models, and the even-even N=Z nuclei between A=68 and 100 play a dominant role.

The work of F. R., Ch. F., and F.-K. T was supported by the Swiss National Science Foundation grant 20-47252.96. T. R.

acknowledges support by an APART fellowship from the Austrian Academy of Sciences. H. S. was supported by the German Academic Exchange Service (DAAD) with a "Doktorandenstipendium aus Mitteln des zweiten Hochschulsonderprogramms". M. W. was supported by the DOE grant DE-FG02-95-ER40934.

REFERENCES

Arnould, M., Norgaard, H., Thielemann, F.-K., & Hillebrandt, W. 1980, ApJ, 237, 931

Ayasli, A., & Joss, P. C. 1982, ApJ, 256, 637

Biehle, G. T. 1991, ApJ, 380, 167

Biehle, G. T. 1994, ApJ, 420, 364

Cannon, R. C. 1993, MNRAS, 263, 817

Cannon, R. C., Eggleton, P. P., Zytkow, A. N., & Podsiadlowski, P. 1992, ApJ, 386, 206

Champagne, A., & Wiescher, M. 1992, ARN&PS, 42, 39

Coc, A., Mochkovitch, R., Oberto, Y., Thibaud, J.-P., & Vangioni-Flam, E. 1995, A&A, 299, 479

Cowan, J. J., Thielemann, F.-K., & Truran, J. W. 1991, Phys. Rep., 208, 267

Fowler, W. A., Caughlan, G. E., & Zimmermann, B. A. 1967, ARA&A, 5, 525

Fryer, C. L., Benz, W., & Herant, M. 1996, ApJ, 460, 801

Görres, J., & Wiescher, M. 1995, Phys. Rev. C, 52, 412

Görres, J., Wiescher, M., & Thielemann, F.-K. 1995, Phys. Rev. C, 51, 392

Hanawa, T., Sugimoto, D., & Hashimoto, M. 1983, Publ. Astron. Soc. Japan, 35, 491

Herndl, H., Görres, J., Wiescher, M., Brown, B. A., & van Wormer, L. 1995, Phys. Rev. C, 52, 1078

Hoffman, R., Woosley, S. E., Fuller, G. M., & Meyer, B. S. 1996, ApJ, 460, 478

Howard, W. M., Meyer, B. S., & Woosley, S. E. 1991, ApJL, 373, L5

Iliadis, C., Görres, J., Ross, J. G., Schaller, K. W., Wiescher, M., & et al. 1993, Nucl. Phys. A, 559, 83

Kratz, K.-L., Bitouzet, J.-P., Thielemann, F.-K., Möller, P., & Pfeiffer, B. 1993, ApJ, 403, 216

Lewin, W. H. G., van Paradijs, J., & Taam, R. E. 1993, Space Sci. Rev., 62, 223

Meyer, B. S. 1994, ARA&A, 32, 153

Rauscher, T., Thielemann, F.-K., & Kratz, K.-L. 1996, Mem. Soc. Astron. Ital., in press

Rayet, M., Arnould, M., Hashimoto, M., Prantzos, N., & Nomoto, K. 1995, A&A, 298, 517

Ross, J. G., Görres, J., Iliadis, C., Vonzonkas, S., Wiescher, M., & et al. 1995, Phys. Rev. C, 52, 1681

Schatz, H. 1996, to be published

Starrfield, S., Truran, J. W., Politano, M., Sparks, W. M., Nofar, I., & Shaviv, G. 1993, Phys. Rep., 227, 223

Sugimoto, D., & Nomoto, K. 1980, Space Sci. Rev., 25, 155

Taam, R. E., Woosley, S. E., & Lamb, D. Q. 1996, ApJ, 459, 271

Taam, R. E., Woosley, S. E., Weaver, T. A., & Lamb, D. Q. 1993, ApJ, 413, 324

Thielemann, F.-K., Kratz, K.-L., Pfeiffer, B., Rauscher, T., van Wormer, L., & Wiescher, M. 1994, Nucl. Phys. A, 570, 329c

van Wormer, L., Görres, J., Iliadis, C., Wiescher, M., & Thielemann, F.-K. 1994, ApJ, 432, 326

Wallace, R. A., & Woosley, S. E. 1981, ApJS, 45, 389

Wiescher, M., Görres, J., Thielemann, F.-K., & Ritter, H. 1986, A&A, 160, 56

Woosley, S. E., Taam, R. E., & Weaver, T. A. 1986, ApJ, 301, 601

This 2-column preprint was prepared with the AAS LaTeX macros v4.0.

$$\rho=\rho_0(T/T_0)^{4/3},\ T=T_0e^{-t/\tau}$$

$$\tau=120\ \mathrm{s},\quad \rho_0=10^4\ \mathrm{g/cm^3},\quad T_0=0.25\times10^9\ \mathrm{K}$$

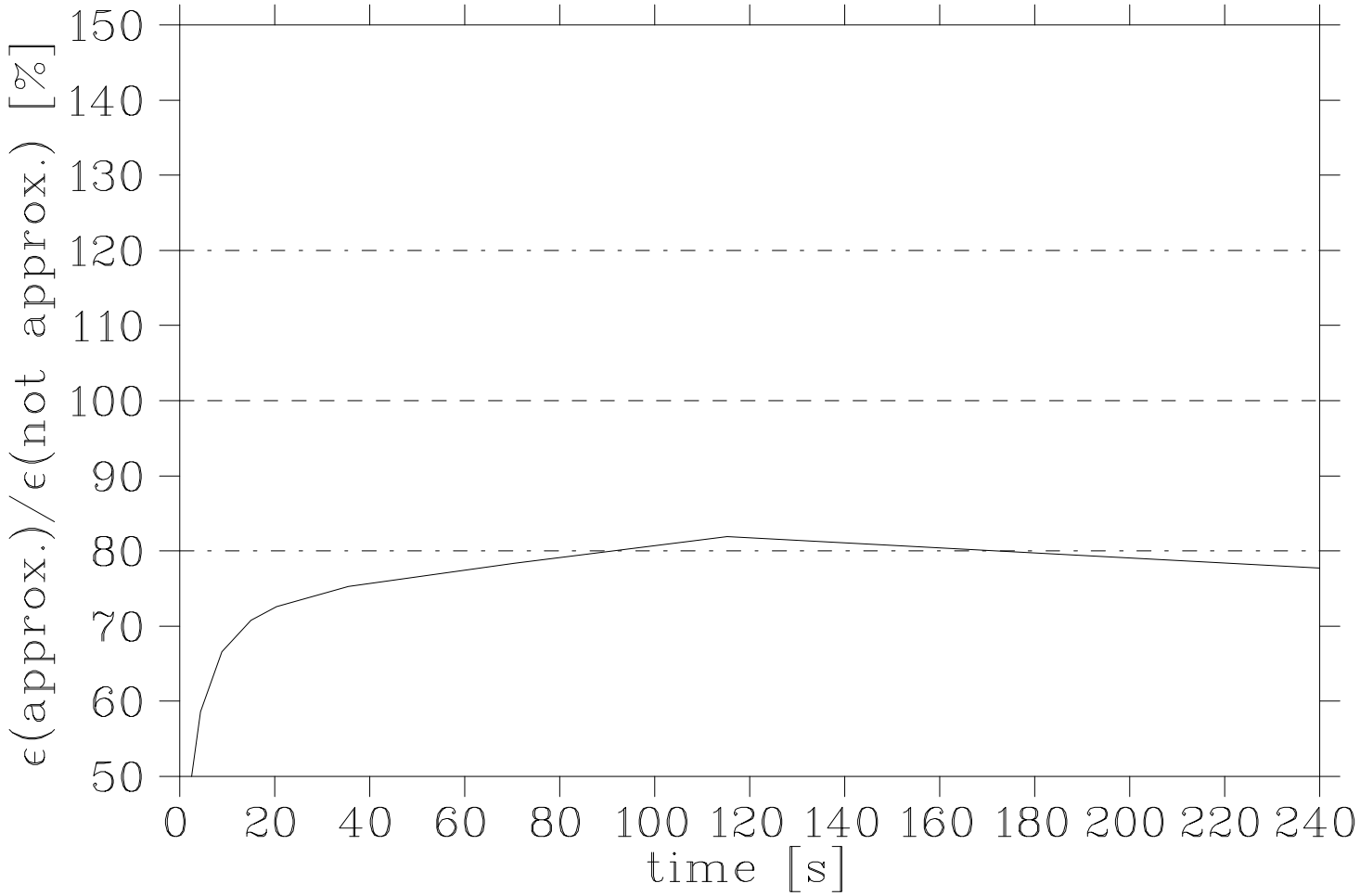

$$\rho=\rho_0(T/T_0)^{4/3},\ T=T_0e^{-t/\tau}$$

$$\tau=1.2\ \mathrm{s},\quad \rho_0=10^6\ \mathrm{g/cm^3},\quad T_0=1.5\times10^9\ \mathrm{K}$$